The Soft Robotic Starfish

Casper Muter, Ansh Mehta, Jennifer Yeo, John Roger Finnerty, Demetrios Kechris

***Abstract*— The "Soft Robotic Starfish" project showcases a bio-inspired robot designed for the Spring 2024 Robosoft competition in the ME568 Soft Robotics course. Utilizing soft pneumatic actuators, origami bellows, and granular jamming, this robot mimics starfish locomotion, adapting to complex environments. Fabrication involved cost-effective materials, and functionality was validated through FEA simulations and empirical testing. The project highlights soft robotics' potential in improving flexibility and safety for applications like search-and-rescue and human-robot interaction.**

I. Introduction

In the rapidly evolving field of robotics, the exploration of soft robotics has opened new avenues for designing machines that are flexible, adaptable, and capable of interacting safely with humans and delicate environments. This project "The Soft Robotic Starfish," displays the innovation and potential in soft robotics. This project focuses on developing a soft robotic system leveraging soft pneumatic actuators and innovative origami-based design.

This paper will delve into the design, manufacturing, and testing phases of the Soft Robotic Starfish, discussing the theoretical models used for simulation and the empirical outcomes observed through rigorous testing. The discussion aims to highlight how soft robotics can revolutionize fields such as search-and-rescue, remote sensing, and human-robot interaction, presenting a versatile platform for future robotic innovations.

II. Prior Works

Soft robotics proposes many unique advantages over traditional rigid robots including, increased resistance to damage, performance in unstructured environments, and safer interaction with humans and the environment [4]. Soft bio inspired robots have been explored because of the ability of animals to move in complex environments due to the deformability of their soft structures [2]. The soft robotic starfish has been investigated previously by many researchers including Shepherd *et al* from Harvard University [7]. While this design has the capability to locomote at low pressures and varying gaits, it was not previously examined whether this robot could locomote in varying environments or have the capability to manipulate objects [7]. Additionally, a quadrupedal soft robotic starfish using a tendon based mechanism was explored; while this robot was compact, had the ability to locomote in various directions, and could be controlled wirelessly at a certain distance, the body was fabricated using poly lactic acid (PLA) [5]. This design is more rigid than the proposed soft robotic starfish in this paper, and tendon based mechanisms can have the tendency to cause failure of the robot due to polymer tear and cable breakage [3]. There has also been research into shape memory alloy (SMA) soft robotic starfish, in which the robot could traverse over obstacles and in varying environments, with different gaits such as rolling, crawling, creeping, navigating, and bypassing; however the use of SMA springs have a longer actuation time that that of the pneumatic actuators proposed [9]. For the proposed robots in this paper, there were three main components including, soft pneumatic actuators, inflatable origami bellows, and variable stiffening mechanisms. Soft pneumatic actuators have often been used because of their low cost, light weight, fast response time, and easy implementation [10]. Inflatable origami bellows have been investigated because of their unique ability to create a 3D shape from 2D shapes, and help apply a force to the desired object or location [6]. Lastly, there have been many variable stiffening mechanisms developed with the main purpose of conforming to and manipulating objects without crushing them - often times with these graspers able to reliably hold objects with forces exceeding their weight [1].

III. Intellectual Merit

Our work makes the following contributions in demonstrating the unique capabilities of soft robotics.

- We demonstrate two different methods of locomotion without traditional means such as motorized joints.
- We've built general purpose robots that are robust to a wide range of environmental conditions and physical wear.
- We've demonstrated jamming-based graspers which offer a promising new means of general-purpose compliant grasping that is cheap and doesn't require any precise control.

IV. Design and Manufacturing

A. Soft Robotic Starfish

The design process for the soft robot began with creating molds for the body and legs using SolidWorks. The leg designs drew inspiration from Harvard's pneunet design[7], incorporating minor modifications to enhance functionality. The body mold was designed with a hexagonal shape, ensuring that four of its sides matched the top length of the legs for seamless integration. The CAD models for these parts are show in Figures 1 and 2.

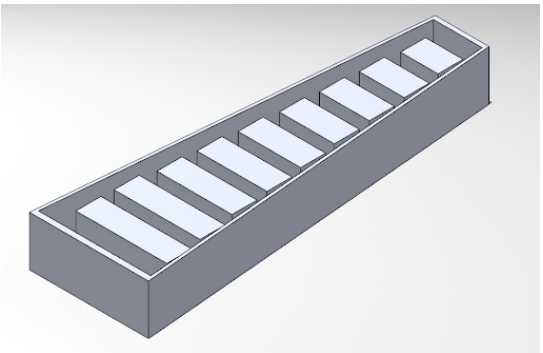

Fig. 1. Starfish Leg CAD Model

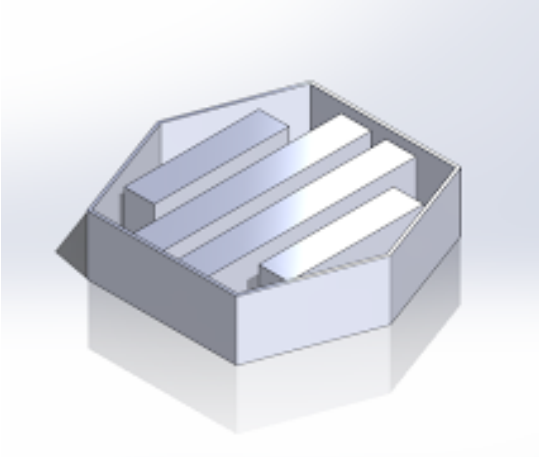

Fig. 2. Starfish Body CAD Model

To optimize locomotion, the attachment angles of the legs were adjusted at the front and rear, enabling the front legs to effectively propel the robot forward. A FormLabs 3D resin printer was used to produce the molds, utilizing resin material capable of withstanding high temperatures (up to 70 degrees Celsius). This characteristic is essential, as traditional PLA or SLA materials typically deform under such thermal conditions.

With the molds ready, assembly of the robot commenced. The process began by adding 30 grams of DragonSkin silicone to the leg mold, followed by using 35 grams to fill the body mold. Due to limited printer availability, only one leg mold was initially printed, which prolonged the manufacturing process. After all molds were prepared, a layer of DragonSkin was spincoated on an acrylic plate, and a fabric layer was added to act as a strain limiter on the still-uncured silicone. Another layer of uncured polymer was then applied over this, followed by the placement of the molds. The assembly was cured at 70 degrees Celsius for 15 minutes.

Post-curing, an X-ACTO knife was used to trim the molds to the appropriate size. The robot's body was then prepared by applying uncured DragonSkin to the areas designated for leg attachment and carefully positioning the legs. This assembly was baked at 70 degrees Celsius for another 15 minutes. Holes were cut for the tubing, the tubes were inserted, and sealed with Silpoxy to complete the construction of the soft robot.

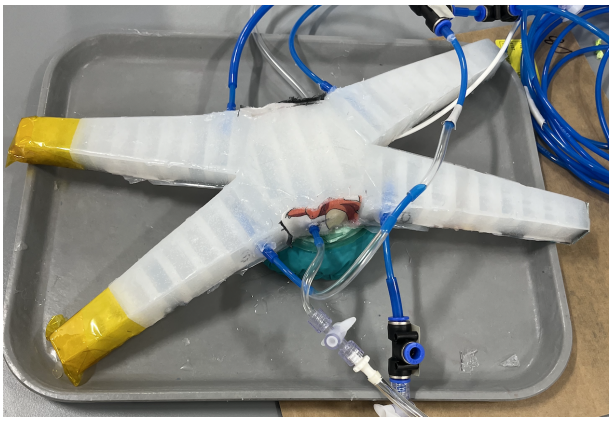

Fig. 3. Completed Starfish

Teflon tape (yellow) was wrapped around the ends of the front legs in order to facilitate sliding. Ski skin fabric was applied to the tips of the rear legs to enable directional friction - these skin created resistance allowing the legs to push the robot forward (during reverse actuation), but didn't apply any resistance when the legs were actuating in the forward direction (inflating).

B. Soft Robotic Wheel

For the first iteration of the wheel, there were 6 independent pneumatic chambers (Figure 4). The CAD model was fused deposition modeling (FDM) printed using polylactic acid (PLA).

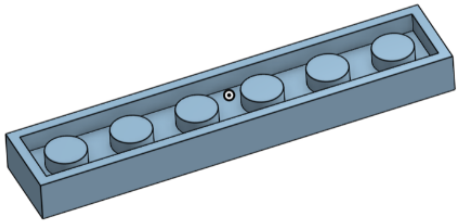

Fig. 4. CAD model of verison 1 of the soft pneumatic wheel top mold

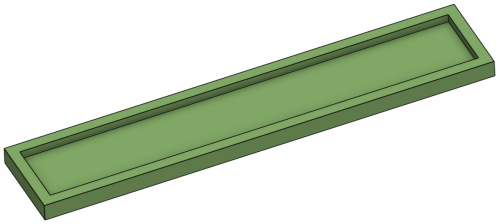

Fig. 5. CAD model of the soft pneumatic wheel bottom mold

About 150 mL of DragonSkin 10 was mixed with equal amounts of Part A and Part B, and poured into the chamber

mold. The leftover DragonSkin 10 was poured into the bottom mold and a fabric layer was added for strain limiting (Figure 5 and 6). Two molds were cured at room temperature for 5 hours minimum. Once the two halves were cured and removed from the molds, another layer of DragonSkin 10 was added to adhere the two layers together. The fabricated silicone strip was turned into a wheel by forming a circular shape using tape and adding DragonSkin 10 to adhere the two edges. However, this process actually created an oblong shape which made it difficult to roll well. Tubing was added to the soft wheel prototyped for testing. During initial testing, it was clear that there were too many pneumatic lines and connectors that weighed down the wheel and restricted locomotion. bottom mold.

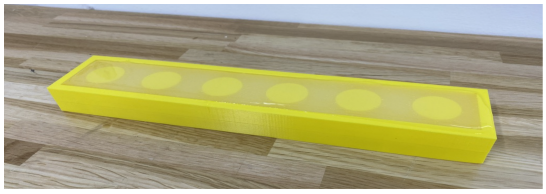

Fig. 6. Molding the soft pneumatic wheel using the top mold

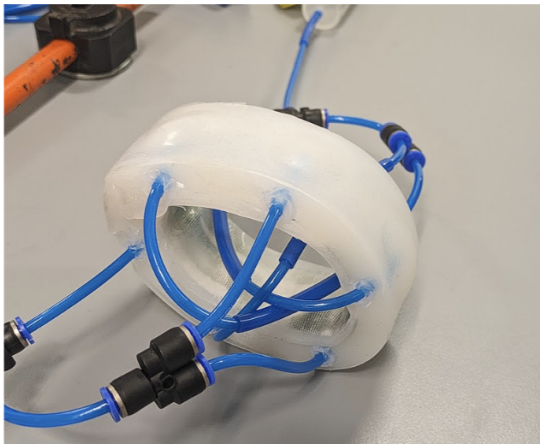

Fig. 7. Wheel Version 1 Prototype

The second iteration of the wheel design incorporated channels to create two groups of three connected pneumatic chambers (Figure 8). In addition, chamfers on the ends of the mold were incorporated to improve the process of turning the flat strip into a circular wheel shape. A simple silicone body mold of dimensions 3in by 4in by 1.5 in was also created using cardboard. The same process as described previously for molding was used for this second iteration. A fixture was used to turn the flat strip into a circular shape. After two soft wheels, and one body had been fabricated, they were assembled together using DragonSkin 10. While this second iteration was able to locomote better with the reduction of tubing and connections, the wheel still had difficulty rolling. This may be attributed to a variety of issues including: fabrication errors, leaks in the system, number of chambers, and the method of connecting the chambers.

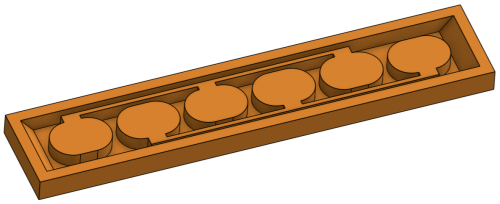

Fig. 8. CAD model of verison 2 of the soft pneumatic wheel top mold

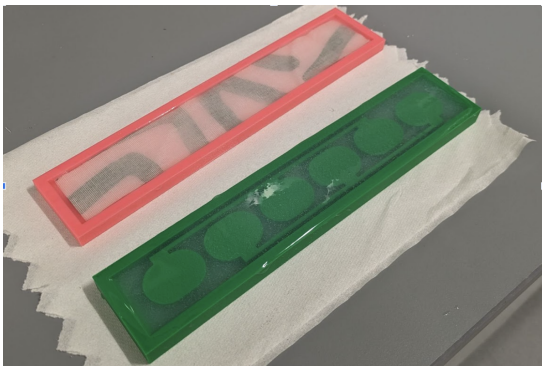

Fig. 9. Molding the soft pneumatic wheel using the molds

C. TPE Bellows

The purpose of the bellows was to increase the amount of force the jamming grasper can apply on an object. To create a 4 bellow stack, the layers of thermoplastic elastomer (TPE) and the masking layer (parchment paper) were first designed in Onshape (Figure 11). The films were designed to have four corner holes for alignment pins. The films were cut using a CO2 laser cutter, and the layers were aligned and stacked onto heat press plates as shown in Figure 12. The heat press plates were used to supply heat at 290F, and at a force of 250 lbf for 12 minutes to the bellow stack for bonding the layers. The excess parts of the bellow stack were cut away to leave just the bellow shape, and the bellows were able to be pressurized with air for actuation (Figure 13).

D. Jamming Grasper

Initially, the jamming grasper was created using a TPE outer pouch filled with ground coffee. However, it was difficult to maintain a proper vacuum due to leaks during the manufacturing stage, especially when adding tubing to the pouch. In addition, the TPE did not seem to stretch as much which made it more difficult to conform to a 3D object. A latex balloon was swapped for the TPE pouch to allow for better conformability to an object as well as increased friction. While the latex balloon worked better than the TPE pouch, the overall jamming grasper was still too small and too firm to pick up larger and heavier objects. A third prototype was made from a balloon and lentils, replacing the finely ground coffee. The expectation was that the larger granular material would allow heavier objects to be lifted. For the fourth prototype, an XL latex glove was used as the

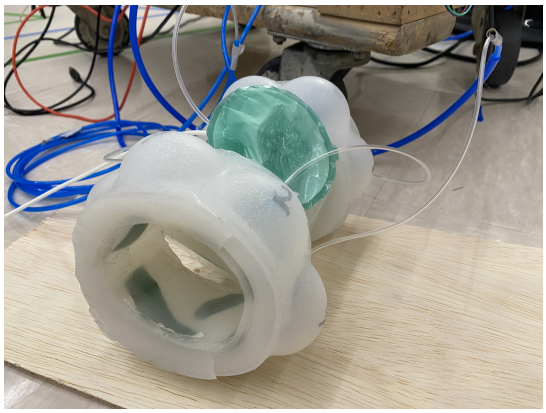

Fig. 10. Wheel Version 2 Prototype

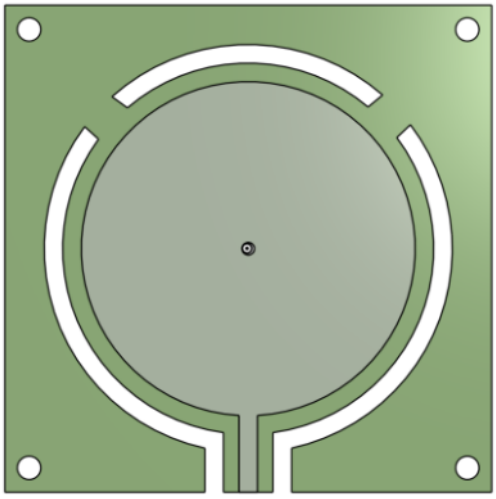

Fig. 11. CAD model of bellow film layers

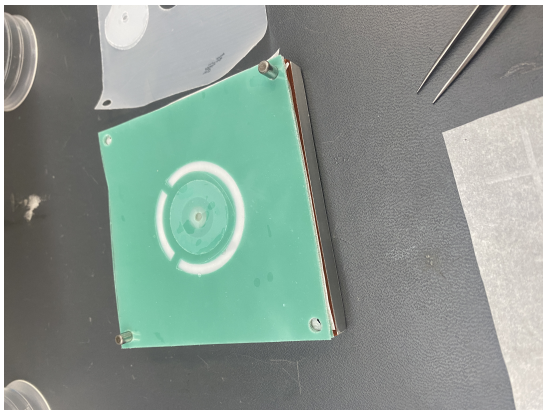

Fig. 12. Bellows after heat pressing

Fig. 13. Bellows Actuated

outer pouch. The fingers of the glove were closed off and the glove was filled with lentils. The grain size of the lentils were larger than that of the ground coffee which allowed for a softer grasper and better conformability to objects.

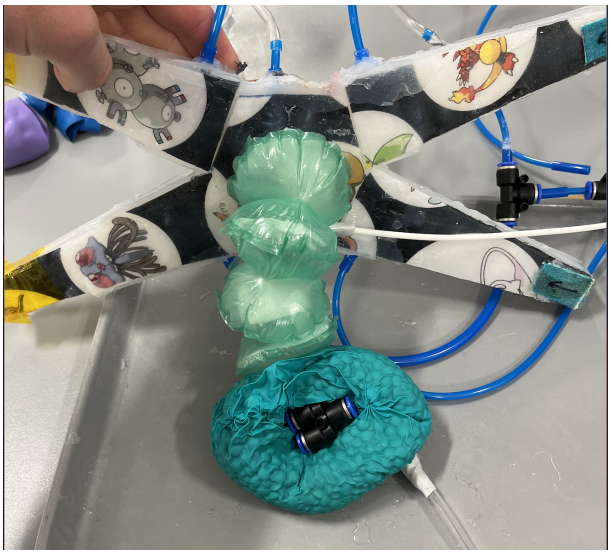

Fig. 14. Starfish with Bellows, Grasping an Object

V. Modeling Component

A finite element analysis (FEA) simulation was conducted using Abaqus to model the internal stress and forces when the legs of the robot are actuated. First, a CAD model was created for the molded part, as well as two simple slab shapes that match the area of the bottom of the leg. These were needed to model the strain limiting layer and the thin layer of polymer outside of it. The Dragon Skin material was modeled using the Yeoh hyperelastic [11] model, according to Equation (1).

$$W = \sum_{i=1}^{3} C_i (I_1 - 3)^i \tag{1}$$

Like all hyperelastic models, the Yeoh equation models the strain energy density W, the amount of elastic energy

stored in a unit volume of material under a stretched state described by the principal stretches λ_1, λ_2, and λ_3 [8]. These values are equal to the ratio of the deformed to initial length along the three principal axes and I_1 is the first principal invariant, equal to $\lambda_1^2 + \lambda_2^2 + \lambda_3^2$. They Yeoh model is chosen for materials with large deformations, typically over 400%, which is applicable for our robot. The coefficients C_1, C_2, and C_3 were provided by [8], with units of MPa.

C_1	C_2	C_3
0.036	0.00025	0.000023

TABLE I

YEOH MODEL COEFFICIENTS

The fabric was modeled as an isotropic material using the linear elastic model ($E = \sigma\epsilon$) with the following values.

Young's Modulus	Poisson's Ratio
6500	0.2

TABLE II

FABRIC MATERIAL PARAMETERS

The assembly was constrained in all directions at the base and a gravitational load was applied. A pressure of 60 kPa was applied uniformly on the inner cavity surface of the leg. The part was meshed with quadratic tetrahedral elements and the loading simulation was run, resulting in the deformation shown in Figure 15.

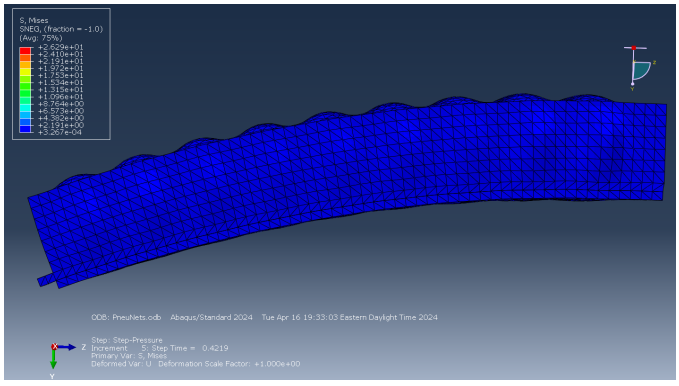

Fig. 15. Abaqus Load Simulation of Starfish Leg, Side View

Results from the load simulation are included in Table III.

Pressure (MPa)	Max von Mises Stress (MPa)
0.06	2.191

TABLE III

FEA SIMULATION RESULTS

These results informed the pressure that the robot limbs require for desired operation.

VI. TESTING AND VALIDATION OF FUNCTIONALITY

A. Controls and Sensing

The robot required a robust control interface, with rapid iteratibility, so that the gait and control strategy for the robots could be developed in a short amount of time. For this purpose, we used 2 SMC ITV003s and 2 SMC ITV005s to regulate positive pressure from 100KPa to 10,000 KPa. and 100KPa to 50,000KPa respectively, using a 0-10V Analog Signal, along with a SMC ITV009 to regulate the amount of negative pressure from -1 to -100 KPa. The Analog Signal was provided by using an I2C addressable DAC Module from DFRobot, which was controlled using a ESP32. Each DAC Module was configured to use a different address, reducing the amount of wiring involved. The ESP32 was configured to receive Hexadecimal commands from the serial port, in the format given by Table IV.

Field	**Value**
Magic Byte	0x02
Channel Number	0xCC
Pressure (Lower Byte)	0xLL
Pressure (Higher Byte)	0xHH
CRC	XOR of Channel Number and Pressure

TABLE IV

COMMAND BYTES

A Python function was written to script the bytes being sent to the ESP32 from a computer. The function had the parameters - channel number and pressure percentage.

A pressure sensors within the SMC ITV0000 series regulators allowed for closed loop control of the pressure inside the chambers, with sufficient resolution for pressure control.

B. Validation

We performed various experiments to ensure that the starfish was able to perform it's task. The first tests performed on a freshly finished mold was always a leak test. A small amount of air was pressed into the mold by using a syringe to see if pressure is being maintained in the mold. If there were any leaks that could not be found by sight and feel, that piece was then submerged in water and actuated. The leak would cause bubbles to appear in the bath, allowing for an easy time locating gaps in the silicon.

With no leaks, bending and force tests were performed on the limbs and body to determine maximum bending angles. At maximum actuation, the limbs were had a bending angle of 153 degrees. Actuating the body of the fully assembled starfish caused the limbs to bend 30 degrees. Together this gives the limbs a maximum achievable bending angle of 168 degrees. Using a force sensor, the maximum force provided by each leg was 1651.3 grams of force.

Using the control system, we also determined the actual pressure required to actuate the Starfish legs and body, shown in Table V.

To test different gait, we both manually actuated the limbs with syringes and programs with the control system to see whether each gait was feasible. Multiple gaits were

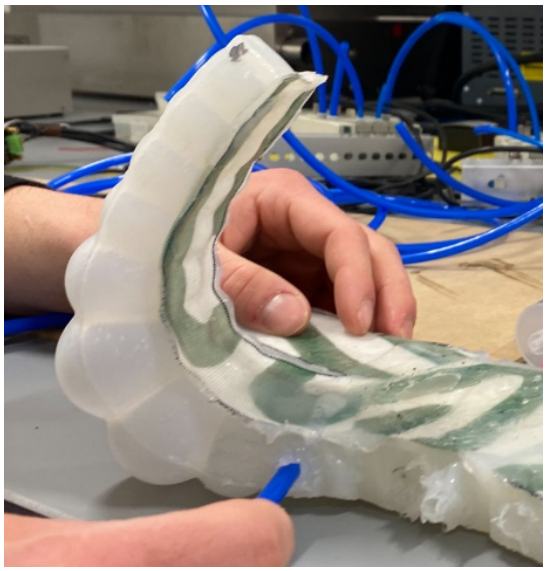

Fig. 16. Limb max bending angle

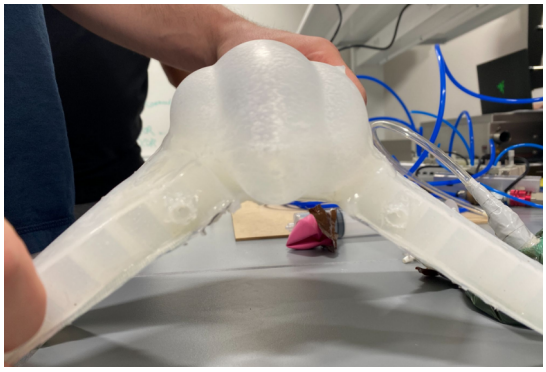

Fig. 17. Body max bending angle

tested, including actuating one leg at a time, alternating legs, matching legs, and an undulation pattern. Of the gaits tested, the undulation pattern utilized by the Harvard paper worked best for our configuration with the gripper [7]. To maximize the speed of the robot in this gait, speed skin was put on the rear limbs and the front limbs were taped. This prevented the rear legs from moving backwards and enabled the front legs to slide forward, giving the robot a top speed of .32 cm per second.

Though many different graspers were created, they all revolved around 4 main designs. The first design was a TPE pouch filled with coffee grounds. The second design was a balloon filled with coffee grounds. The third design switched out the coffee grounds in the balloon for lentils. The fourth and final design used an extra large latex glove filled with lentils. All of the grapsers were tested in the same way, attempting to pick up pneumatic junctions, pens, and small weights. To test the gripper, we filled it slightly with air, pressed it onto an object, and vacuumed the air out to jam the granules inside before lifting the gripper up.

The first design (TPE and coffee grounds) did not perform well in tests. Manufacturing it was very difficult, and even

Component	Pressure (MPa)
Body	≈ 0.003
Front Legs (tied together)	≈ 0.005
Back Legs	≈ 0.002 each
Vacuum	-0.001

TABLE V

PRESSURE DISTRIBUTION IN VARIOUS COMPONENTS

when assembled correctly and without leaks it was very hard to get a solid seal on objects to pick them up. Despite our best efforts, it was not able to hold onto even a small weight for longer than a second. On the second design, the change to the latex balloon helped to provide a nicer surface to pick up objects. The coffee grounds did a decent job of conforming to the object, allowing us to grasp some objects securely, albeit inconsistently. It was no trouble to pick up a small object the granular material could envelop and conform, but larger objects would fall right out. To fix this, the coffee grounds were swapped out for lentils in the third prototype. With the lentils, the grasper was able to pick up larger objects, but not as well when picking up the smaller objects. After much experimentation and research, it was deduced that the balloon was causing the problem. Since the balloon is meant to inflate to a large volume of a predefined shape, it has a large elastic force that needed to be overcome to deform it from that predefined shape. Simply, the balloon was too stiff to properly deform and pick objects up, though both designs were able to hold 200 g. For the fourth prototype, an extra large latex glove was filled with lentils. The glove provided a strong, yet easily deformable surface that allowed the lentils to easily mold to the desired object. This grasper was able to securely pick up both small and large objects, picking up the maximum tested weight of 200 grams with ease.

The final test performed on the robots was the drop test, a simple test to ensure durability. The robot is raised to a height and dropped onto the ground, then tested to see if it is able to actuate correctly. Individual limbs and the entirety of both the starfish and wheel were tested in the drop test at a maximum height of 2 meters. The stiffest parts of the design are the tubing and grippers, and if a failure occurred it would likely be at either of these two points. Fortunately, both robots succeeded in the drop test with minimal damage and were able to locomote away.

VII. CONCLUSION

Two soft robots were designed and tested by navigating challenging environments that traditional hard robots may struggle in. They are designed using two different methods of locomotion without traditional means such as motorized joints. A meticulously general-purpose compliant jamming grasper that is cheap and doesn't require precision control allows both the starfish and wheel to easily grasp objects of varying sizes and carry them securely. The highly durable Dragonskin-10 silicon body makes it resilient and able to withstand falls from up to two meters without damage. With further design and testing, this design may be able to assist

in search-and-rescue efforts, remote sensing, and create safer human-robot interaction.

REFERENCES

[1] Eric Brown, Nicholas Rodenberg, John Amend, Annan Mozeika, Erik Steltz, Mitchell R. Zakin, Hod Lipson, and Heinrich M. Jaeger. Universal robotic gripper based on the jamming of granular material. *Proceedings of the National Academy of Sciences*, 107(44):18809–18814, 2010.

[2] Stephen Coyle, Carmel Majidi, Philip LeDuc, and K. Jimmy Hsia. Bio-inspired soft robotics: Material selection, actuation, and design. *Extreme Mechanics Letters*, 22:51–59, 2018.

[3] Useok Jeong, Keunsu Kim, Sang-Hun Kim, Hyunhee Choi, Byeng Dong Youn, and Kyu-Jin Cho. Reliability analysis of a tendon-driven actuation for soft robots. *The International Journal of Robotics Research*, 40(1):494–511, 2021.

[4] Chiwon Lee, Myungjoon Kim, Yoon Kim, Nhayoung Hong, Seungwan Ryu, and Sungwan Kim. Soft robot review. *International Journal of Control, Automation and Systems*, 15, 01 2017.

[5] M. Munadi, Mochammad Ariyanto, Joga D. Setiawan, and M. Fikri Al Ayubi. Development of a low-cost quadrupedal starfish soft robot. In *2018 5th International Conference on Information Technology, Computer, and Electrical Engineering (ICITACEE)*, pages 225–229, 2018.

[6] T. Ranzani, S. Russo, F. Schwab, C. J. Walsh, and R. J. Wood. Deployable stabilization mechanisms for endoscopic procedures. In *2017 IEEE International Conference on Robotics and Automation (ICRA)*, pages 1125–1131, 2017.

[7] Robert Shepherd, Filip Ilievski, Wonjae Choi, Stephen Morin, Adam Stokes, Aaron Mazzeo, Xin Chen, Michael Wang, and George Whitesides. Multigait soft robot. *Proceedings of the National Academy of Sciences of the United States of America*, 108:20400–3, 11 2011.

[8] Matheus S Xavier, Andrew J Fleming, and Yuen K Yong. Finite element modeling of soft fluidic actuators: Overview and recent developments. *Advanced Intelligent Systems*, 3(2):2000187, 2021.

[9] Matheus S. Xavier, Charbel D. Tawk, Ali Zolfagharian, Joshua Pinskier, David Howard, Taylor Young, Jiewen Lai, Simon M. Harrison, Yuen K. Yong, Mahdi Bodaghi, and Andrew J. Fleming. Soft pneumatic actuators: A review of design, fabrication, modeling, sensing, control and applications. *IEEE Access*, 10:59442–59485, 2022.

[10] Matheus S. Xavier, Charbel D. Tawk, Ali Zolfagharian, Joshua Pinskier, David Howard, Taylor Young, Jiewen Lai, Simon M. Harrison, Yuen K. Yong, Mahdi Bodaghi, and Andrew J. Fleming. Soft pneumatic actuators: A review of design, fabrication, modeling, sensing, control and applications. *IEEE Access*, 10:59442–59485, 2022.

[11] OH Yeoh. Hyperelastic material models for finite element analysis of rubber. *Journal of Natural Rubber Research*, 12(1997):142–153, 1997.